Photonic band gaps of AB_3 and B_3 structures of metallodielectric spheres

Photonic band gaps of AB_3 and B_3 structures of metallodielectric spheres

Anan Fang, Weiyi Zhang, Zhenlin Wang, An Hu and Naiben Ming

National Laboratory of Solid State Microstructures and Department of Physics,
Nanjing University, Nanjing 210093, China

Abstract

Using the vector-wave multiple-scattering method we have calculated the photonic band structures of AB_3 and B_3 crystals composed of perfect metal spheres in air. It is shown that AB_3 photonic crystal contains a large photonic band gap and B_3 photonic crystal has more than one gap when the filling ratio of metal spheres exceeds a threshold. The multiple photonic gaps of the B_3 structure are useful in the design of optical multi-channel perfect mirrors and optical multi-band filters in the microwave regime.

Photonic band-gap (PBG) crystals are dielectric materials where the dielectric constant is modulated periodically in either one, two, or all three spatial directions. The variation of the dielectric constant affects the propagating behaviours of the corresponding Bloch waves; the strongest influence occurs near the Brillouin boundaries where travelling waves are transformed into standing waves, and this results in photonic band gaps. The existence of photonic band gaps has attracted much attention in recent years because of their vast potential for applications [1–5]; it also provides new ways to control light propagation and underlying physical processes. There are possible applications in suppression of electron–hole recombination [1], perfect mirrors, optical band filters, and production of high-efficiency lasers [6, 7].

For most crystals, there is only one gap in the band structure. That is to say, there is one perfect mirror, and that is only for a specific frequency. It is inconvenient and uneconomical to use such an optical mirror. In this paper we propose theoretically using photonic crystals of B_3 structure (figure 1(b)) composed of perfect metal spheres in air to manufacture an optical mirror. The advantage of using such a structure is that there are multiple photonic band gaps; this feature leads to an important application in making optical multi-band filters that can work for more than one specific frequency.

To fabricate PBG crystals, the following two techniques are widely adopted: (1) micro-electronic fabrication techniques [8–10]; (2) synthetic opal/inverse-opal synthesis technologies [11–16]. By using such techniques, photonic crystals at microwave length scales are not difficult to make. However, the fabrication of photonic crystals at optical length scales is
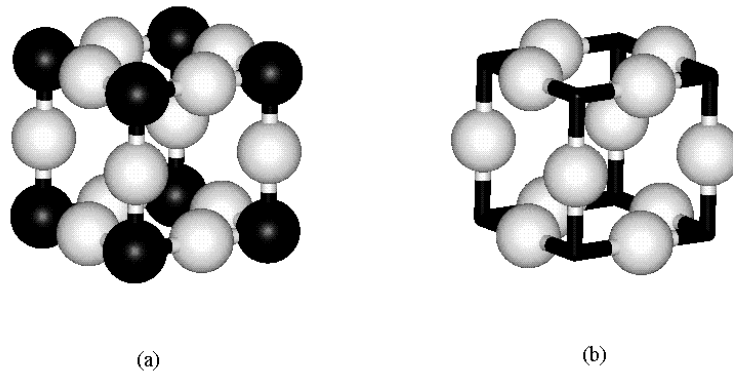
(a) (b)

Figure 1. The crystal structures: (a) AB$_3$ structure; (b) B$_3$ structure.

rather difficult and significant progress has been made only recently. For conventional dielectric photonic crystals, the opening of a full photonic band gap depends very much on the global symmetry of the crystal structure. Theoretical studies and experimental investigations show that only a few of them have a complete band gap; notable examples are the diamond structure with high-dielectric-constant spheres embedded in a low-dielectric-constant background and the face-centred cubic structure made using inverse-opal techniques.

In addition to the conventional photonic crystals, photonic crystals with metal components have also been attracting more attention in the last few years [17–26]. Both theoretical and experimental studies have shown that any structure composed of metal or multiply coated spheres each with an inner metal layer (such as FCC, BCC, and SC structures) can give a complete photonic band gap [20, 25, 26] if the filling ratio exceeds a threshold. The size and frequency of the photonic gap is determined by the filling ratio and the local configuration rather than the crystal symmetry and long-range order [25, 26].

In this paper, we have calculated the photonic band structures of a new crystal type—the AB$_3$ structure (figure 1(a)) of perfect metal spheres in air. This structure is chosen because it has four spheres per primitive cell, and large variation in the dielectric constant in space can be realized by using different combinations of A and B spheres. It is shown that a large photonic band gap exists in the AB$_3$ structure for a wide range of ratios between the A and B radii. The photonic gap is large enough to compensate for the loss due to the boundary effect of the finite crystal. Also, in the microwave regime, samples of AB$_3$ photonic crystals are not difficult to fabricate.

The calculation below is based on the well-established vector-wave multiple-scattering theory (MST) for electromagnetic waves (see e.g. references [27–31]). The method is also called the vector-wave KKR approach. The scalar-wave multiple-scattering method was originally developed long ago for electronic band-structure calculations for solids, where electrons are described by scalar wavefunctions. The extension of the multiple-scattering method to vector waves was carried out independently by Ohtaka [27], Lamb *et al* [28], Wang *et al* [30], Modinos [29], and Moroz [31], and applied to study a variety of properties of electromagnetic waves. The nice feature of the MST method is the separation of the pure geometrical structure factor of the lattice and the scattering properties of the spheres. The photonic band structures can be obtained by solving the following secular equations:

$$\text{Det} \left| \delta_{ss'} \delta_{ll'} \delta_{mm'} \delta_{\sigma\sigma'} - \sum_{l''m''\sigma''} G^{ss'}_{lm\sigma,l''m''\sigma''}(\vec{k}) t^{s'}_{l''m''\sigma'',l'm'\sigma'} \right| = 0. \tag{1}$$

Note that $G^{ss'}$ does not include the $s = s'$ term. Here, (l, m) are the angular momentum indices and s is the index of the scatterer in the primitive cell. $t^{s'}_{lm\sigma,l'm'\sigma'}$ is the scattering T-matrix element for the spheres. $G^{ss'}_{lm\sigma,l'm'\sigma'}(\vec{k})$ are the Fourier transforms of the geometrical structure factors $G^{ij}_{lm\sigma,l'm'\sigma'}(\vec{R})$ ($\vec{R} = \vec{R}_i - \vec{R}_j$):

$$G^{ss'}_{lm\sigma,l'm'\sigma'}(\vec{k}) = \sum_{\vec{R}}{}' \mathrm{e}^{-\mathrm{i}\vec{k}\cdot\vec{R}} G^{ij}_{lm\sigma,l'm'\sigma'}(\vec{R}). \tag{2}$$

$G^{ij}_{lm\sigma,l'm'\sigma'}(\vec{R})$ can be expressed as

$$G^{ij}_{lm\sigma,l'm'\sigma'}(\vec{R}) = \begin{cases} \displaystyle\sum_{\mu} C(l1l, m - \mu\mu) g^*_{lm-\mu,l'm'-\mu}(\vec{R}) \\ \qquad \times\, C(l'1l', m' - \mu\mu) & (\sigma = \sigma') \\[2ex] \displaystyle\sqrt{\frac{2l'+1}{l'+1}} \sum_{\mu} C(l1l, m - \mu\mu) g^*_{lm-\mu,l'-1m'-\mu}(\vec{R}) \\ \qquad \times\, C(l' - 11l', m' - \mu\mu) & \sigma = m, \sigma' = e) \\[2ex] \displaystyle -\sqrt{\frac{2l'+1}{l'+1}} \sum_{\mu} C(l1l, m - \mu\mu) g^*_{lm-\mu,l'-1m'-\mu}(\vec{R}) \\ \qquad \times\, C(l' - 11l', m' - \mu\mu) & (\sigma = e, \sigma' = m) \end{cases} \tag{3}$$

where the Cs are the Clebsch–Gordon coefficients and g is the scalar geometrical structure factor given by

$$g_{lm,l'm'}(\vec{R}) = 4\pi \sum_{l''m''} \mathrm{i}^{l'+l''-l} C_{lm;l'm';l''m''} h^{(1)}_{l''}(\kappa R) Y_{l''m''}(-\vec{R}).$$

$\kappa = \omega/c$ and $C_{lm;l'm';l''m''}$ is the Gaunt coefficient. $h^{(1)}_l$ and Y_{lm} are Hankel functions of the first kind and spherical harmonic functions, respectively. In our calculations, the cut-off angular momentum is set as $L_{max} = 7$. Such a cut-off is sufficient for obtaining the desired precision for the given range of frequencies.

In this paper, we concentrate on the band structures of AB$_3$ and B$_3$ photonic crystals of metal spheres in air (see figure 1). The dielectric function for metals is approximately given by $\epsilon(\omega) = 1 - \omega_p^2/\omega^2$ where ω_p is the plasmon frequency. When the photon frequency is higher than the plasmon frequency ω_p, the dielectric constant is positive. The dielectric contrast between the metal spheres and air background is small, so the overall photonic structures resemble the free-photon band structures in vacuum. However, the situation becomes quite different when the photon frequency is far below the plasmon frequency; then the dielectric constant takes a large negative value and electromagnetic waves cannot penetrate into the metal spheres. Such exclusion of electromagnetic waves from the metal spheres restricts the photon propagation modes which favours the formation of photonic band gaps. From the values of dielectric constants listed in [32], it is found that the infrared frequency range corresponds roughly to the dielectric constant $\epsilon = -200$ while the dielectric constant takes a more negative value, $\epsilon = -3900$, when the frequency falls into the microwave range. Another factor that one has to bear in mind is the metal absorption. From the same listing in [32], one notices that the metal absorption can pose serious problems in the infrared frequency range and only a good metal like silver does not affect the gap drastically [24]. But the absorption becomes negligibly small when the frequency is in the microwave regime. As we shall see later, the photonic band gap does not sensitively depend on the value of ϵ if it exceeds a threshold value.

We choose $\epsilon = -200$ in most of our calculations. For comparison, we also present some of the band structures that were obtained using $\epsilon = -3900$. All band structures are given in units of reduced frequency $\omega a / 2\pi c$, where a is the lattice constant and c is the velocity of light in vacuum.

Before presenting detailed numerical results, we would like to discuss the physical mechanism of formation of the photonic band gap in photonic crystals made of metal spheres. For photonic crystals composed of metal spheres embedded in a medium, the volumes surrounded by neighbouring spheres form connected cavities. The frequencies of cavity modes and separations among modes are inversely proportional to the sizes of the cavities. Therefore, increasing the filling ratio has two impacts on the band-gap formation:

(1) the channels between neighbouring cavities become narrow, which reduces the coupling among the modes in neighbouring cavities; thus the cavity-mode-induced bandwidths are also reduced;

(2) the size of each cavity also gets reduced, which enhances the separations among modes in the cavity.

These two opposite effects determine a critical filling ratio where the band gap starts to appear. As the filling ratio increases further, the size of the gap increases until the spheres touch each other. This is the origin of the opening of the lowest gap in the band structures. However, the appearance of other gaps depends very much on the crystal symmetry, the material components of the spheres, and the filling ratio. Thus, to create more than one gap, an appropriate structure must be chosen.

In figure 2, we show the calculated photonic band structures of AB_3 crystals composed of metal spheres of one type in air. The filling ratio of the spheres is 0.26. There is a large absolute gap between the R point in the dielectric band (the second band) and the X point in the air band (the third band). The gap/mid-gap ratio ($\Delta\omega/\omega_{mid}$) approaches 34%. It is important for applications to have a high gap/mid-gap ratio to compensate for the boundary effect of actual crystals. The value of the gap/mid-gap ratio must be larger than 5% in order to be useful. Note that the photonic band structures obtained using $\epsilon = -200$ (figure 2(a)) and $\epsilon = -3900$
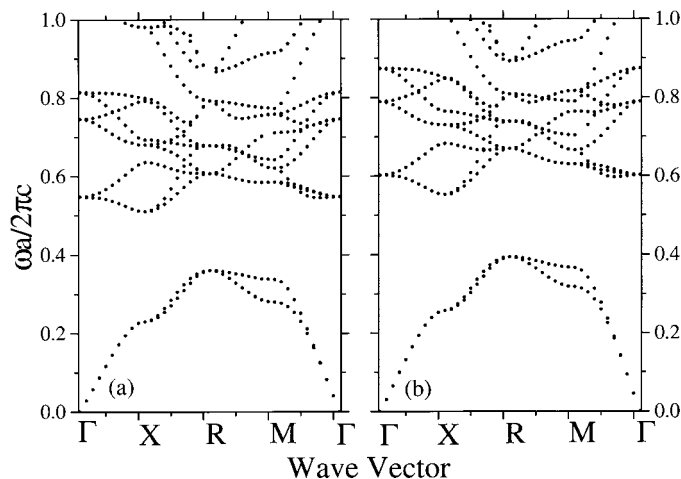

Figure 2. The photonic band structures of AB_3 crystals composed of metal spheres of one type in air. The filling ratio is $f = 0.26$. The dielectric constant of the spheres is: (a) $\epsilon = -200$; (b) $\epsilon = -3900$.

(figure 2(b)) are almost the same except that figure 2(b) is raised slightly in comparison with figure 2(a) because of the shorter penetration length in the latter case. This makes the effective size of the cavities in the latter smaller than that in the former. The dependence of the gap size on the filling ratio f is shown in figure 3. The size of the gap increases as the filling ratio of spheres increases beyond a certain threshold (0.215). The upper gap edge increases a little, but the lower gap edge declines dramatically because of rapid shrinking of the bandwidth with f.
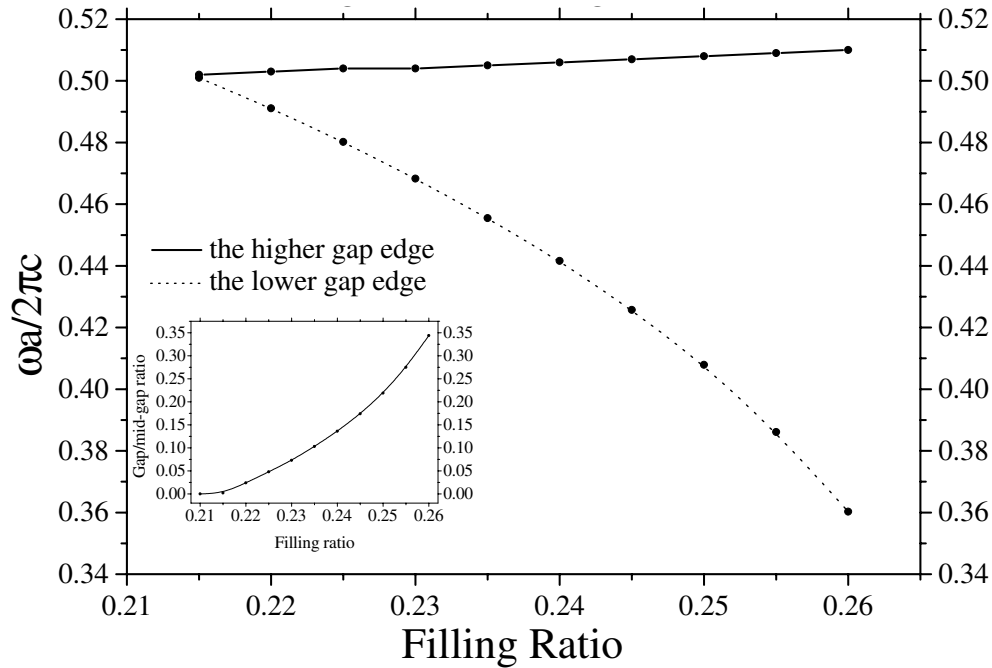

Figure 3. The gap size as a function of the filling ratio f for AB$_3$ crystals. The inset gives the dependence of the gap/mid-gap ratio on the filling ratio f. Here, $\epsilon = -200$.

We also calculated the band structure of AB$_3$ crystals where metal spheres A and B have different radii, but are nearly touching. The gap size as a function of the ratio r_a/r_b (where r_a and r_b are the radii of spheres A and B, respectively) is given in figure 4. The ratio varies from 0.42 to 30; the gap is found to be robust over the whole range studied. When the ratio r_a/r_b is relatively large, only one gap exists. This can be understood from the structure of AB$_3$ crystals shown in figure 1(a). One sees that there are wide channels among neighbouring cavities. They lead to strong coupling among the modes in those cavities inscribed by neighbouring spheres. When the ratio is relatively small, the cavities are less connected, so the coupling is weak enough for new gaps to open. Figure 5 gives the band structure of AB$_3$ crystal where the ratio r_a/r_b equals 0.42. In this case, the spheres are very closely packed and there are three gaps in the band structure. From bottom to top, their gap/mid-gap ratios are 24.6%, 9.8%, and 6.1%, respectively. This example shows that for some structures, more than one gap can appear as the filling ratio increases.

This novel feature is also present in B$_3$ photonic crystals where A spheres are all removed from the AB$_3$ structure. The band structures are shown in figure 6. The filling ratio of the spheres f is 0.51, which is slightly smaller than the close-packed value 0.555. The use of a small filling ratio is important in actual applications, because this can prevent the contact of metal spheres, with the result that long-range currents cannot be formed and the dissipation
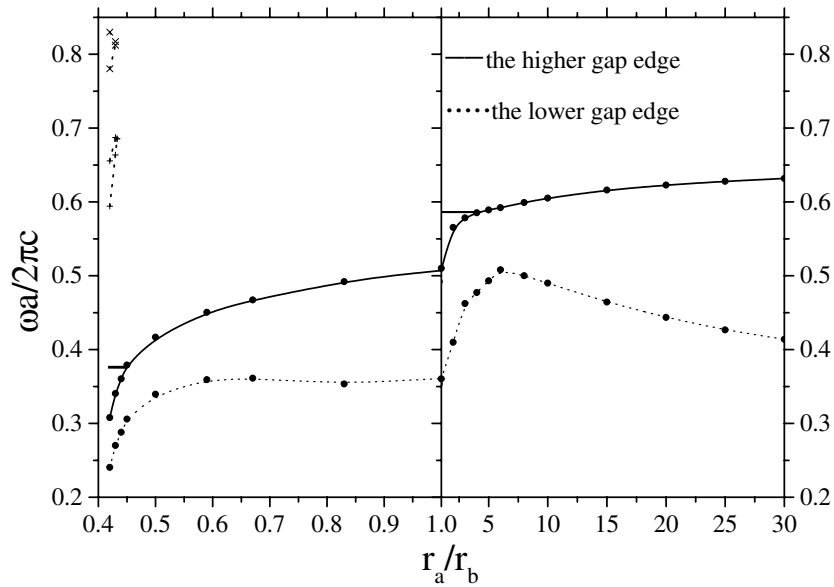
Figure 4. The gap size as a function of the ratio r_a/r_b for AB$_3$ crystals. A and B spheres are nearly touching; $\epsilon = -200$.
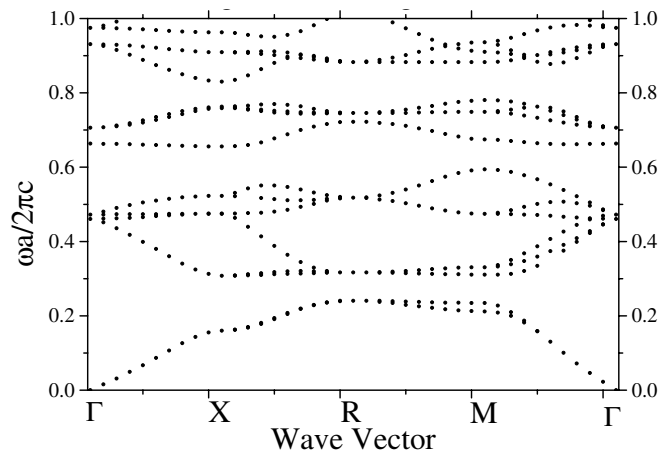

Figure 5. The photonic band structure of AB$_3$ crystal at $r_a/r_b = 0.42$ and $\epsilon = -200$.

can be minimized. There are also three gaps in the band structures. From bottom to top, their gap/mid-gap ratios are 10%, 5.1%, and 6.0%. From the B$_3$ structure shown in figure 1(b), we see that the channels among the neighbouring spheres are very narrow. Note that here again similar band structures are obtained for the dielectric constants $\epsilon = -200$ (figure 6(a)) and $\epsilon = -3900$ (figure 6(b)). In figure 7, the dependence of the gap as a function of the filling ratio f is given. As the filling ratio increases, the channels become narrower and the sizes of the gaps increase. When the size exceeds a certain value, a narrow band appears between the second and third gaps. The feature of having more than one gap can be used in the design of some important optical devices, such as an optical multi-band filters and optical multi-channel perfect mirrors, at least in the microwave frequency range.
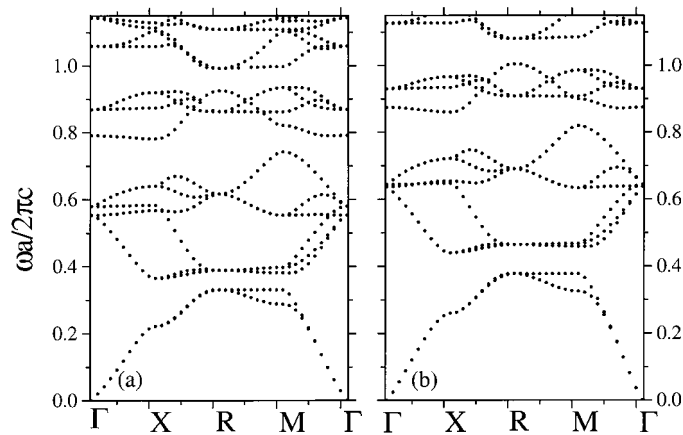
Figure 6. The photonic band structures of B$_3$ crystals composed of metal spheres in air. The filling ratio is $f = 0.51$. The dielectric constant of the spheres is: (a) $\epsilon = -200$; (b) $\epsilon = -3900$.
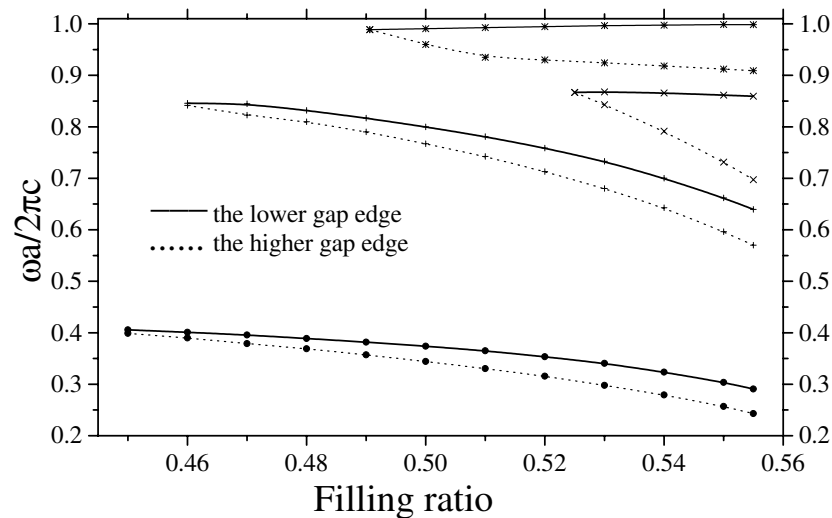

Figure 7. The gap size as a function of the filling ratio f for B$_3$ crystals. Here, $\epsilon = -200$.

In summary, the photonic band structure of AB$_3$ crystal can contain a large gap over a wide range of the ratio r_a/r_b. For the B$_3$ structure, up to four gaps can be present over a certain range of the filling ratio. This feature can be used in the design of an optical multi-channel filter or an optical multi-channel perfect mirror in the microwave regime.

Acknowledgments

References

[1] Yablonovitch E 1987 *Phys. Rev. Lett.* **58** 2059
[2] John S 1987 *Phys. Rev. Lett.* **58** 2486
[3] Yablonovitch E, Gmitter T J and Blat R 1988 *Phys. Rev. Lett.* **61** 2546
[4] Joannopoulos J D, Meade R D and Winn J N 1995 *Molding the Flow of Light* (Princeton, NJ: Princeton University Press)
[5] Soukoulis C M (ed) 1996 *Photonic Band Gap Materials (NATO Advanced Study Institute Series E: Applied Sciences, vol 315)* (Dordrecht: Kluwer)
[6] Lin Shawn-Yu, Fleming J G, Chow E, Bur J, Choi K K and Goldberg A 2000 *Phys. Rev.* B **62** 2243
[7] Nojima S 2000 *Phys. Rev.* B **61** 9940
[8] Lin S Y *et al* 1998 *Nature* **394** 251
[9] Fleming J G and Lin S Y 1999 *Opt. Lett.* **24** 49
[10] Noda S and Sasaki A 1997 *Japan. J. Appl. Phys.* **36** 1907
[11] Wijnhoven J E G and Vos W L 1998 *Science* **281** 802
[12] van Blaaderen A 1998 *Science* **282** 887
[13] Velev A, Jede T A, Lobo R F and Lenhoff A M 1997 *Nature* **389** 448
[14] Zakhidov A *et al* 1998 *Science* **282** 897
[15] Holland B T, Blanford C F and Stein A 1998 *Science* **281** 538
[16] Subramania G *et al* 1999 *Appl. Phys. Lett.* **74** 3933
[17] Brown E R and McMahon O B 1995 *Appl. Phys. Lett.* **67** 2138
[18] Sigalas M M, Chan C T, Ho K M and Soukoulis C M 1995 *Phys. Rev.* B **52** 11 744
[19] Sievenpiper D F, Sickmiller M E and Yablonovitch E 1996 *Phys. Rev. Lett.* **76** 2480
[20] Fan S, Villeneuve P R and Joannopoulos J D 1996 *Phys. Rev.* B **54** 11 245
[21] Kuzmiak V and Maradudin A A 1997 *Phys. Rev.* B **55** 7427
[22] Sievenpiper D F, Yablonovitch E, Winn J N, Fan S, Villeneuve P R and Joannopoulos J D 1998 *Phys. Rev. Lett.* **80** 2829
[23] Yannopapas V, Modinos A and Stefanou N 1999 *Phys. Rev.* B **60** 5359
[24] Moroz A 1999 *Phys. Rev. Lett.* **83** 5274
[25] Zhang W Y, Lei X Y, Wang Z L, Zheng D G, Tam W Y, Chan C T and Sheng Ping 2000 *Phys. Rev. Lett.* **84** 2853
[26] Chan C T, Zhang W Y, Wang Z L, Lei X Y, Zheng Dagui, Tam W Y and Sheng P 2000 *Physica* B **279** 150
[27] Ohtaka K 1980 *J. Phys. C: Solid State Phys.* **13** 667
[28] Lamb W, Wood D M and Ashcroft N W 1980 *Phys. Rev.* B **21** 2248
[29] Modinos A 1987 *Physica* A **141** 575
[30] Wang X D, Zhang X G, Yu Q L and Harmon B N 1993 *Phys. Rev.* B **47** 4161
[31] Moroz A 1995 *Phys. Rev.* B **51** 2068
[32] Johnson P B and Christy R W 1972 *Phys. Rev.* B **6** 4370
Johnson P B and Christy R W 1974 *Phys. Rev.* B **9** 5056
Ordal M A *et al* 1983 *Appl. Opt.* **22** 1099